Scale-Space workshop, ICCV 2001, Vancouver, Canada, July 2001.

Down-Scaling for Better Transform Compression

Alfred M. Bruckstein*, Michael Elad, and Ron Kimmel*

JiGami Research Division–Israel

Abstract. The most popular lossy image compression method used on the Internet is the JPEG standard. JPEG's good compression performance and low computational and memory complexity make it an attractive method for natural image compression. Nevertheless, as we go to low bit rates that imply lower quality, JPEG introduces disturbing artifacts. It appears that at low bit rates a down–scaled image when JPEG compressed visually beats the high resolution image compressed via JPEG to be represented with the same number of bits.
Motivated by this idea, we show how down–sampling an image to a low resolution, then using JPEG at the lower resolution, and subsequently interpolating the result to the original resolution can improve the overall PSNR performance of the compression process. We give an analytical model and a numerical analysis of the sub-sampling, compression and re-scaling process, that makes explicit the possible quality/compression trade-offs. We show that the image auto-correlation can provide good estimates for establishing the down-sampling factor that achieves optimal performance. Given a specific budget of bits, we determine the down sampling factor necessary to get the best possible recovered image in terms of PSNR.

1 Introduction

The most popular lossy image compression method used on the Internet is the JPEG standard. JPEG uses the Discrete Cosine Transform (DCT) on image blocks of size 8×8 pixels. The fact that the JPEG operates on small blocks is motivated by the non-stationarity of the image, and the need to approximate the Karhunen Loeve Transform (KLT) for 2D Markov processes. A quality measure determines the (uniform) quantization steps for each of the 64 DCT coefficients. The quantized coefficients of each block are then zigzag-scanned into one vector that goes through a run-length coding of the zero sequences, thereby clustering long insignificant low energy coefficients into short and compact descriptors. Finally, the run-length sequence is fed to an entropy coder, that can be a Huffman coding algorithm with either a known dictionary or a dictionary extracted from the specific statistics of the given image. A different alternative supported by the standard is arithmetic coding.

JPEG's good compression performance and low computational and memory complexity make it an attractive method for natural image compression. Nevertheless, as we go to low bit rates that imply lower quality, the JPEG compression algorithm introduces disturbing artifacts. It appears that at low bit rates a down–scaled image when

* Also affiliated with the Department of Computer Science, Technion–Israel Institute of Technology, Technion City, Haifa 32000, Israel.

M. Kerckhove (Ed.): Scale-Space 2001, LNCS 2106, pp. 123–136, 2001.

JPEG compressed and later interpolated, visually beats the high resolution image compressed directly via JPEG using the same number of bits. An experimental result displayed in Figure 1 shows that both visually and in terms of the Mean Square Error (or PSNR), one obtains better results using down-scaling compression and up-scaling after the decompression.

Fig. 1. Original image (on the left) JPEG compressed–decompressed image (middle), and down-scaled–JPEG compressed-decompressed and up scaled image (right). The down scaling factor - 0.5. In both cases, the compression ratio is 40. The MSE in the upper row is 219.5 (left) and 193.12 (right). Similarly, in the lower row: 256.04 (left) and 248.42 (right).

In this paper we propose an analytical explanation to the above phenomenon, along with a practical algorithm to automatically choose the optimal scaling factor for best PSNR. We derive an analytical model of the compression– decompression reconstruction error as a function of the memory (bits) budget, the (statistical) characteristics of the image, and the scale factor. We show that a simplistic second order statistical model provides a good estimate of the down-sampling factor that achieves optimal performance.

This report is organized as follows. Sections 2–3–4 present the analytic model, and explore its implications. Section 5 describes an experimental setup that validates the proposed model and its applicability for choosing best scaling factor for a given image with a given bits budget. Finally, Section 6 ends the paper with some concluding remarks.

2 Analysis of a Continuous "JPEG-Style" Image Representation Model

In this section we start building a theoretical model for analyzing the expected reconstruction error when doing compression–decompression as a function of the total bits budget, the characteristics of the image, and the scale factor. Our model considers the image over a continuous domain rather then a discrete one, in order to simplify the derivation. The steps we follow are:

- Derivation of the expected compression-decompression error for a general image representation process, based on slicing the image domain into M by N blocks.
- Derivation of an expression for the error by exploiting the fact that the coding is done in the transform domain using an orthonormal basis, and assuming that the error is due only to truncating the transform coefficients.
- Extension of the expression for the error to include quantization error of the non-truncated coefficients.
- Extension of the formal error to take into account the fact that the transform is the DCT, i.e. the orthonormal basis is cosine functions.
- Including in the expression for the error an approximation of the quantization errors due to various policies of allocation the total bits budget.

At the end of this process we obtain an expression for the error as a function of the bits budget, scale factor, and the image characteristics. This function eventually allows us to determine the optimal scale–down factor in JPEG-like image coding.

2.1 Compression-Decompression Expected Error

Assume we are given images on the unit square $[0,1]\times[0,1]$, $f_w(x,y):[0,1]\times[0,1]\rightarrow \mathbf{R}$, realizations of a 2D random process $\{f_w(x,y)\}$, with second order statistics given by

$$E(f_w(x,y))=0, \qquad \mathcal{R}(x,y;x+\tau_x,y+\tau_y)=r_0^2 e^{-\alpha_x|\tau_x|}e^{-\alpha_y|\tau_y|}.$$

We assume that the image domain $[0,1]\times[0,1]$ is sliced into $M\cdot N$ regions of the form

$$\Delta_{ij}\equiv\left[\frac{i-1}{M},\frac{i}{M}\right]\times\left[\frac{j-1}{N},\frac{j}{N}\right] \quad \text{for} \quad i=1,2,..,M; j=1,2,..,N,$$

Assume that due to our coding of the original image $f_w(x,y)$ we obtain the compressed-decompressed result $\hat{f}_w(x,y)$, which is an approximation of the original image. We can measure the error in approximating $f_w(x,y)$ by $\hat{f}_w(x,y)$ as follows

$$\begin{aligned}\mathcal{E}_w^2 &= \iint_{[0,1]\times[0,1]}(f_w(x,y)-\hat{f}_w(x,y))^2dxdy\\ &=\sum_{i=1}^{M}\sum_{j=1}^{N}\iint_{\Delta_{ij}}(f_w(x,y)-\hat{f}_w(x,y))^2dxdy\end{aligned}$$

$$= \sum_{i=1}^{M}\sum_{j=1}^{N} \text{Area}(\Delta_{ij}) \frac{1}{\text{Area}(\Delta_{ij})} \iint_{\Delta_{ij}} (f_w(x,y) - \hat{f}_w(x,y))^2 dxdy$$
$$= \sum_{i=1}^{M}\sum_{j=1}^{N} \frac{1}{M \cdot N} \left\{ MSE_{f_w}(\Delta_{ij}) \right\},$$

where we define $MSE_{f_w}(\Delta_{ij}) \equiv \frac{1}{\text{Area}(\Delta_{ij})} \int_{\Delta_{ij}} (f_w(x,y) - \hat{f}_w(x,y))^2 dxdy$. We shall, of course, be interested in the expected mean square error of the digitization, i.e.,

$$E(\mathcal{E}_w^2) = \sum_{i=1}^{M}\sum_{j=1}^{N} \frac{1}{M \cdot N} E\left(\frac{1}{\text{Area}(\Delta_{ij})} \iint_{\Delta_{ij}} (f_w(x,y) - \hat{f}_w(x,y))^2 dxdy \right)$$

Note that the assumed wide–sense stationarity of the image process results in the fact that $E(MSE_f(\Delta_{ij}))$ is independent of (i,j), i.e., we have the *same* expected mean square error over each slice of the image. Thus we can write

$$E(\mathcal{E}_w^2) = M \cdot N \frac{1}{M \cdot N} E(MSE_{f_w}(\Delta_{11}))$$
$$= E\left(\frac{1}{\text{Area}(\Delta_{11})} \iint_{\Delta_{11}} (f_w(x,y) - \hat{f}_w(x,y))^2 dxdy \right).$$

Up to now we considered the quality measure to evaluate the approximation of $f_w(x,y)$ in the digitization process. We shall next consider the set of basis functions needed for representing $f_w(x,y)$ over each slice.

2.2 Bases for Representing $f_w(x,y)$ over Slices

In order to represent the image over each slice Δ_{ij}, we have to choose an orthonormal basis of functions. Denote this basis by $\{\Phi_{kl}(x,y)\}_{k,l=0,1,2,\ldots}\}$. We must have

$$\iint_{\Delta_{ij}} \Phi_{kl}\Phi_{k'l'} dxdy = \delta_{kk'}\delta_{ll'} = \begin{cases} 1 \text{ if } (k,l) \equiv (k',l') \\ 0 \text{ otherwise.} \end{cases}$$

If $\{\Phi_{kl}\}$ is indeed a basis, then we can write $f_w(x,y) = \sum_{k=0}^{\infty}\sum_{l=0}^{\infty} \langle f_w(x,y), \Phi_{kl}(x,y)\rangle \Phi_{kl}(x,y)$, as a representation of $f_w(x,y)$ over Δ_{ij} in terms of an infinite set of coefficients

$$F_{kl} \equiv \langle f_w(x,y), \Phi_{kl}(x,y)\rangle = \iint_{\Delta_{ij}} f_w(x,y)\Phi_{kl}(x,y) dxdy.$$

Suppose now that we approximate $f_w(x,y)$ over Δ_{ij} by using only a finite set Ω of the orthonormal functions $\{\Phi_{kl}(x,y)\}$, i.e consider

$$\hat{f}_w(x,y) = \sum\sum_{(k,l)\in\Omega} \langle f_w(x,y), \Phi_{kl}(x,y)\rangle \Phi_{kl}(x,y),$$

(It is easy to see that the optimal coefficients in the approximation above turn out to be the corresponding F_{kl} 's from the infinite representation!). The mean square error of this approximation, over Δ_{11} say, will be

$$MSE_{f_w}(\Delta_{11}) = M \cdot N \left[\iint_{\Delta_{11}} f_w^2(x,y)dxdy \right.$$
$$\left. -2\iint_{\Delta_{11}} f_w(x,y)\hat{f}_w(x,y)dxdy + \iint_{\Delta_{11}} \hat{f}_w^2(x,y)dxdy \right]$$

Hence,

$$MSE_{f_w}(\Delta_{11})$$
$$= M \cdot N \left[\iint_{\Delta_{11}} f_w^2(x,y)dxdy - \sum\sum_{(k,l)\in\Omega} \langle f_w(x,y), \phi_{kl}(x,y)\rangle^2 \right]$$

Now the expected $MSE_{f_w}(\Delta_{11})$ will be:

$$E(MSE_{f_w}(\Delta_{11}))$$
$$= M \cdot N \left[\iint_{\Delta_{11}} E{f_w}^2(x,y)dxdy - \sum\sum_{(k,l)\in\Omega} E\langle f_w(x,y), \phi_{k,l}(x,y)\rangle^2 \right]$$

Hence $E\mathcal{E}_\omega^2 = M \cdot N \cdot r_0^2 \cdot \frac{1}{M \cdot N} - M \cdot N \cdot \sum\sum_{(k,l)\in\Omega} E(F_{kl}^2) = r_0^2 - M \cdot N \cdot \sum\sum_{(k,l)\in\Omega} E[F_{k,l}^2]$.

2.3 The Effect of Quantization of the Expansion Coefficient F_{kl}

Suppose that in the approximation $\hat{f_w}(x,y) = \sum\sum_{(k,l)\in\Omega} F_{kl}\Phi_{k,l}(x,y)$ we can only use a finite number of bits in representing the coefficients$\{F_{kl}\}$ that take values in R. If F_{kl} is represented / encoded with b_{kl} -bits we shall be able to describe it via F_{kl}^Q that takes on $2^{b_{kl}}$ values only, i.e. $F_{kl}^Q = Q_{b_{kl}}(F_{kl}) : R \rightarrow$ set of $2^{b_{kl}}$ representation levels. The error in representing F_{kl} in this way is $\Gamma_{kl}^2 = (F_{kl} - F_{kl}^Q)^2$. Let us now see how the quantization errors affect the $MSE_{f_w}(\Delta_{11})$. We have

$$MSE_{f_w}^Q(\Delta_{11}) = \frac{1}{\frac{1}{M} \cdot \frac{1}{N}} \iint_{\Delta_{11}} \left(f_w(x,y) - \hat{f}_w^Q(x,y) \right)^2 dxdy$$

where $\hat{f}_{w(x,y)}^Q = \sum\sum_{k,l\in\Omega} F_{kl}^Q \phi_{kl}(x,y)$. Now

$$M \cdot N \iint_{\Delta_{11}} \left(f_w(x,y) - \hat{f}_w(x,y) + \hat{f}_w(x,y) - \hat{f}_w^Q(x,y) \right)^2 dxdy$$
$$= MSE_{f_w}(\Delta_{11}) + M \cdot N \cdot \sum\sum_{kl\in\Omega} \Gamma_{kl}^2 = MSE_{f_w}^Q(\Delta_{11}).$$

The expected $MSE_{f_w}^Q(\Delta_{11})$ is therefore given by:

$$E(MSE_{f_w}^Q)(\Delta_{11})$$

$$= r_0^2 - M \cdot N \cdot \sum\sum_{(k,l)\in\Omega} \cdot [F_{k,l}^2] + M \cdot N \sum\sum_{(k,l)\in\Omega} E[F_{kl} - F_{kl}^Q]^2$$

Hence, in order to evaluate $E[\mathcal{E}_w^Q]^2$ in a particular representation when the image is sliced into $M \cdot N$ pieces and over each piece we use a subset Ω of the possible basis functions (i.e. $\Omega \subset \{(k,l)|k,l = 0,1,2..\}$) and we quantize the coefficients with B_{kl}-bits we have to evaluate

$$r_0^2 - M \cdot N \cdot \sum\sum_{(k,l)\in\Omega} \{\text{ variance of } F_{kl}\}$$
$$+M \cdot N \cdot \sum\sum_{(k,l)\in\Omega} \{\text{error in quantizing } F_{kl}\}$$

2.4 An Important Particular Case: Markov Process with Separable Cosine Bases

We have the statistics of $\{f_w(x,y)\}$ given by

$$E(f_w(x,y)) = 0, \quad Ef_w(x,y)f_w(x+\tau_x, y+\tau_y) = r_0^2 e^{-\alpha_x|\tau_x|}e^{-\alpha_y|\tau_y|}$$

and we choose a separable cosine basis for the slices, i.e. over $[0,\frac{1}{M}]\times[0,\frac{1}{N}]$, $\Phi_{kl}(x,y) = \varphi_k(x)\varphi_l(y)$ where $\varphi_k(x) = \sqrt{M(2-\delta_k)}\cos kM\pi x, \quad k = 0,1,2,...,$ and $\varphi_l(x) = \sqrt{N\,(2-\delta_l)}\cos l\,N\,\pi x, \quad l = 0,1,2,....$ To compute $E\mathcal{E}_w^2$ for this case we need to evaluate the variances of F_{kl} defined as $F_{kl} \equiv \int_{\Delta_{11}} f_w(x,y)\varphi_k(x)\varphi_l(y)dxdy$, we have

$$EF_{kl}^2 = E\iint_{\Delta_{11}}\iint_{\Delta_{11}} f_w(x,y)f_w(\xi,\eta)\varphi_k(x)\varphi_l(y)\varphi_k(\xi)\varphi_l(\eta)dxdyd\xi d\eta$$
$$= \iint_{\Delta_{11}}\iint_{\Delta_{11}} r_0^2 e^{-\alpha_x|x-\xi|}e^{-\alpha_y|y-\eta|} \cdot M(2-\delta_k)\cos(k\pi Mx)\cos(k\pi M\xi)$$
$$\cdot N(2-\delta_l)\cos(l\pi Ny)\cos(l\pi Ny)dxdyd\xi d\eta.$$

Therefore, by separating the integrations we obtain

$$EF_{kl}^2 = r_0^2\,(2-\delta_k)\int_0^{\frac{1}{M}}\int_0^{\frac{1}{M}} e^{-\alpha_x|x-\xi|}\cos(k\pi Mx)\cos(k\pi M\xi)Mdxd\xi$$
$$\cdot(2-\delta_l)\int_0^{\frac{1}{N}}\int_0^{\frac{1}{N}} e^{-\alpha_y|y-\eta|}\cos(l\pi Ny)\cos(l\pi N\eta)Ndyd\eta$$

Changing variables of integration to $\tilde{x} = Mx \;\; \tilde{x} \in [0,1], \tilde{\xi} = M\xi \;\; \tilde{\xi} \in [0,1], \tilde{y} = Ny \;\; \tilde{y} \in [0,1]$, and $\tilde{\eta} = N\eta \;\; \tilde{\eta} \in [0,1]$ yields

$$EF_{kl}^2 = r_0^2(2-\delta_k)(2-\delta_l)\cdot\frac{1}{M}\cdot\int_0^1\int_0^1 e^{-\frac{\alpha_x}{M}|\tilde{x}-\tilde{\xi}|}\cos(k\pi\tilde{x})\cos(k\pi\tilde{\xi})d\tilde{x}d\tilde{\xi}$$
$$\cdot\frac{1}{N}\int_0^1\int_0^1 e^{-\frac{\alpha_y}{N}|\tilde{y}-\tilde{\eta}|}\cos(l\pi\tilde{y})\cos(l\pi\tilde{\eta})d\tilde{y}d\tilde{\eta}$$

Let us define, for compactness, the following integral: $\int_0^1\int_0^1 e^{-A|x-\xi|}\cos(k\pi x)\cos(l\pi\xi)dxd\xi \equiv \mathcal{M}(A;k,l)$ Then we see that

$$EF_{kl}^2 = r_0^2(2-\delta_k^D)\cdot\frac{1}{M}\cdot\mathcal{M}(\frac{\alpha_x}{M};k,k)\cdot(2-\delta_l^D)\cdot\frac{1}{N}\cdot\mathcal{M}(\frac{\alpha_y}{N};l,l)$$

We have that

$$\mathcal{M}(A;k,l) = (1+\delta_k^D \text{ or } {}_l)\delta_{|k-l|}^D \frac{A}{A^2+k^2\pi^2}$$
$$-\left(1+(-1)^{l+k}\right)\frac{A^2}{(A^2+(l\pi)^2)(A^2+(k\pi)^2)}\cdot\frac{(2-e^{-A}[(-1)^k+(-1)^l])}{2}$$

Therefore some algebra yields

$$EF_{kl}^2 = \frac{4r_0^2}{M\cdot N}\left[\frac{(\frac{\alpha_x}{M})}{(\frac{\alpha_x}{M})^2+k^2\pi^2}\right]\left(1-(2-\delta_k^D)(1-(-1)^k e^{-(\frac{\alpha_x}{M})})\frac{(\frac{\alpha_x}{M})}{(\frac{\alpha_x}{M})^2+k^2\pi^2}\right)\cdot$$
$$\cdot\left[\frac{(\frac{\alpha_y}{N})}{(\frac{\alpha_y}{N})^2+l^2\pi^2}\right]\left(1-(2-\delta_l^D)(1-(-1)^l e^{-(\frac{\alpha_y}{N})})\frac{(\frac{\alpha_y}{N})}{(\frac{\alpha_y}{N})^2+l^2\pi^2}\right).$$

2.5 Incorporating the Effect of Coefficient Quantization

We have that $E[F_{kl}-F_{kl}^Q]^2 \sim \mathcal{K}\cdot\frac{\text{Var}\{F_{kl}\}}{2^{2b_{kl}}}$, where $\mathcal{K}$ is a constant in the range $[1,3]$. According to rate-distortion theory (for uniform and Gaussian variables) the above formula for evaluating the error due to quantization describes well the behavior of the error as a function of the number of bits allocated for representing F_{kl}.

Putting the above results together, we get that the expected mean square error in representing images from the process $\{f_w(x,y)\}$ with Markov statistics, by slicing the image plane into $M\cdot N$ slices and using, over each slice, a cosine basis is given by:

$$E[\mathcal{E}_w^Q]^2$$
$$= r_0^2\left\{1-\sum\sum_{k,l\in\Omega}(2-\delta_k^2)(2-\delta_l^2)\ \mathcal{M}(\frac{\alpha_x}{M};k,k)\mathcal{M}(\frac{\alpha_y}{N};l,l)\ [1-\frac{\mathcal{K}}{2^{2b_{kl}}}]\right\}$$

This expression gives $E[\mathcal{E}_w^Q]^2$ in terms of $r_0, \{\alpha_x,\alpha_y\}$ and $\{b_{kl}\}$ - the bits allocated to the coefficients $F_{kl}$where the subset of the coefficient is given via Ω.

3 The Slicing and Bit–Allocation Optimization Problems

Suppose we consider

$$E[\mathcal{E}_w^Q]^2$$
$$= r_0^2\left\{1-\sum\sum_{k,l\in\Omega}(2-\delta_k^D)\ \mathcal{M}(\frac{\alpha_x}{M};k,k)(2-\delta_l^D)\mathcal{M}(\frac{\alpha_y}{N};l,l)\ [1-\frac{\mathcal{K}}{2^{2b_{kl}}}]\right\}$$

as a function of $M,N,\{b_{kl}\}$. We have that the total bit usage in representing the image is

$$B_{\text{TOT}} = \left(\sum\sum_{k,l\in\Omega} b_{kl}\right)\cdot M\cdot N$$

Now we can solve a variety of bit–allocation and slicing optimization problems.

3.1 Optimal Local Bit Allocation and Slicing Given Total Bit Usage

Given the constraint

$$\sum\sum_{(k,l)\in\Omega} b_{kl} = \frac{B_{\text{TOT}}}{M\cdot N},$$

find $\{b^*_{kl}\}$ that minimize the $E\mathcal{E}^2_w$. We need to minimize

$$\sum\sum_{k,l\in\Omega} \overbrace{(2-\delta^D_k)\mathcal{M}(\frac{\alpha_x}{M};k,k)(2-\delta^D_l)\mathcal{M}(\frac{\alpha_y}{N};l,l)\mathcal{K}}^{\tilde{\sigma}^2_{kl}} 2^{-2b_{kl}}.$$

This is a classical bit allocation process and we have that the optimal bit allocation yields (theoretically) the same error for all terms in

$$\sum\sum_{k,l\in\Omega}\frac{\tilde{\sigma}^2_{kl}}{2^{2b_{kl}}} = \sum\sum_{k,l\in\Omega}\frac{\tilde{\sigma}^2_{kl}}{\Lambda^2_{kl}}$$

where we defined Λ_{kl} as the number of quantization levels, see [6]. Hence we need

$$\frac{\tilde{\sigma}^2_{kl}}{\Lambda^2_{kl}} = \text{Const} \Rightarrow \Lambda^2_{kl} = \frac{\tilde{\sigma}^2_{kl}}{\text{Const}}$$

and we should have $2^{2\sum\sum b_{kl}} = \prod_{kl\in\Omega}\Lambda^2_{kl} = 2^{2B_{TOT}/(MN)}$. The result is

$$b_{kl} = \frac{1}{2}\log_2\tilde{\sigma}^2_{kl} + \frac{B_{\text{TOT}}}{M\cdot N}\cdot\frac{1}{|\Omega|} - \frac{1}{2}\log_2(\prod_{(kl)\in\Omega}\tilde{\sigma}^2_{kl})^{\frac{1}{|\Omega|}}$$

With this optimal bit allocation the expression $\sum\sum_{(k,l)\in\Omega}\frac{\tilde{\sigma}^2_{kl}}{2^{2b_{kl}}}$ is minimized to

$$|\Omega|\cdot\text{Const} = |\Omega|\cdot 2^{\frac{-2B_{\text{TOT}}}{M\cdot N}}\left(\prod_{(kl)\in\Omega}\tilde{\sigma}^2_{kl}\right)^{\frac{1}{|\Omega|}}.$$

Hence,

$$E([\mathcal{E}^Q_w]^2)_{OPT} = r_0^2\Bigg\{1 - \sum\sum_{k,l\in\Omega}(2-\delta^D_k)(2-\delta^D_l)\mathcal{M}(\frac{\alpha_x}{M};k,k)\mathcal{M}(\frac{\alpha_y}{N};l,l)$$
$$+|\Omega|2^{\frac{-2B_{\text{TOT}}}{M\cdot N}\cdot\frac{1}{|\Omega|}}\left(\prod_{(k,l)\in\Omega}\mathcal{K}\cdot(2-\delta^D_k)(2-\delta^D_l)\mathcal{M}(\frac{\alpha_x}{M};k,k)\mathcal{M}(\frac{\alpha_y}{N};l,l)\right)^{\frac{1}{|\Omega|}}\Bigg\}$$

an error expression in terms of (B_{TOT}, M, N, Ω) and the second–order–statistics parameters r_0, α_x, α_y of the $\{f_w(x,y)\}$–process.

3.2 Effect of Slicing with Rigid Relative Bit Allocation

An alternative bit allocation strategy perhaps more in the spirit of the classical JPEG standard can also be thought of. Consider that Ω is chosen and the b_{kl}'s are also chosen a-priori for all $(k,l) \in \Omega$. Then we have

$$E[\mathcal{E}_w^Q]^2$$
$$= r_0^2 \left\{ 1 - \sum\sum\nolimits_{k,l\in\Omega} (2-\delta_k^D)(2-\delta_l^D)\mathcal{M}(\frac{\alpha_x}{M};k,k)\mathcal{M}(\frac{\alpha_y}{N};l,l)[1-\frac{\mathcal{K}}{2^{2b_{kl}}}] \right\}$$

as a function of M and N. This function clearly decreases with increasing M and N since more and more bits are allocated to the image, and here $B_{TOT} = M \cdot N \cdot \sum\sum_{k,l\in\Omega} b_{kl}$. Suppose now that for $M = N = 1$, we choose a certain bit allocation for a given Ω (say $\Omega = \{(k,l)|k+l \leq Limit\,, k,l = 0,1,2...\}$) i. e. we chose $\bar{b}_{kl}$ but now as we increase the number of slices (i.e. increase M and N) we shall modify the b_{kl}'s to keep B_{TOT} a constant by choosing $b_{kl}(M,N) = \bar{b}_{kl} \cdot \frac{1}{M \cdot N}$. Here B_{TOT} remains a constant and we can again analyze the behavior of $E[\mathcal{E}_w^Q]^2$ as M and N vary.

3.3 Soft Bit Allocation with Cost Functions for Error and Bit Usage

We could also consider cost functions of the form $C_{MSE}(E[\mathcal{E}_W^Q]^2) + C_B(M \cdot N \cdot \text{Bits/slice})$, where C_{MSE} and C_B are cost functions chosen according to the task in hand, and ask for the bit allocation that minimize the joint functionals, in the spirit of [5].

4 The Theoretical Predictions of the Model

In the previous sections we proposed a model for the compression error as a function of the image statistics $(r_0, \alpha_x, \alpha_y)$, the given total bits budget B_{TOT}, and the number of slicings M and N. Here, we fix these parameters according to the behaviour of natural images and typical compression setups and study the behaviour of the theoretical model.

Assume we have a gray scale image of size 512×512 with 8 bits/pixel, as our original image. JPEG considers 8×8 slices of this image and produces, by digitizing the DCT transform coefficients with a predetermined quantization table, approximate representation of these 8×8 slices. We would like to explain the observation that down-scaling the original image, prior to applying JPEG compression to a smaller image, produces with the same bit usage, a better representation of original image.

Suppose the original image is regarded as the 'continuous' image defined over the unit square $[0,1] \times [0,1]$, as we have done in the theoretical analysis. Then, the pixel width of a 512×512 image will be $1/512$. We shall assume that the original image is a realization of a zero mean 2D stationary random process with autocorrelation of the form

$$\mathcal{R}(|i-i'|,|j-j'|) = r_0^2 |\rho_1|^{|i-i'|} |\rho_2|^{|j-j'|},$$

with ρ_1, and ρ_2 in the range of $[0.8, 0.9]$, as is usually done (see [6]). From a single image, r_0^2 can be estimated via the expression

$$r_0^2 \approx \frac{1}{512 \times 512}(\sum_{i,j}(I(i,j) - \bar{I})^2) = 2\frac{1}{256}(\sum_{0}^{127} i^2) = 32,385.00,$$

assuming an equalized histogram. If we consider that $\rho^{|i-i'|} \cong e^{-\alpha|\frac{i}{512} - \frac{i'}{512}|} = e^{-\frac{\alpha}{512}|i-i'|}$, we can obtain an estimate for α using $e^{-\frac{\alpha}{512}} = \rho \in [0.8, 0.9]$. This provides

$$-\frac{\alpha}{512} = \log_e \rho \longrightarrow \alpha = -512 \times \log_e \rho \in [50, 150].$$

The total number of bits for the image representation will range from 0.05bpp to about 2.0bpp, hence, B_{TOT} will be between $512 \times 512 \times 0.05 = 13,107$ to $512 \times 512 \times 2 = 524,288$ bits for 512×512 original images. Therefore, in the theoretical evaluations we shall take $\alpha_x, \alpha_y \in [50, 150]$, $r_o = 32500$ for 256 gray level images, with total bit usage between $10,000$ and $1,000,000$.

The symmetric x and y axis slicings considered will be $M, N = 1, 2, ...64$, and we shall evaluate

$$E[\mathcal{E}_w^Q]^2$$
$$\equiv r_0^2 \left\{1 - \sum\sum_{k,l \in \Omega} (2 - \delta_k^D)(2 - \delta_l^D)\mathcal{M}(\frac{\alpha}{M}, k, k)\mathcal{M}(\frac{\alpha}{N}, l, l)[1 - \frac{\mathcal{K}}{\Lambda_{kl}^2}]\right\}$$

with Λ_{kl}s provided by the optimal level allocation

$$\Lambda_{kl}^2$$
$$= (2 - \delta_k^D)(2 - \delta_l^D)\mathcal{M}(\frac{\alpha}{M}, k, k)\mathcal{M}(\frac{\alpha}{M}, l, l)\mathcal{K}(2^{2B_{TOT}/M^2})^{\frac{1}{|\Omega|}} \frac{1}{[\prod_{(k,l)\in\Omega}(\tilde{\sigma}_{kl}^2)]^{\frac{1}{|\Omega|}}}$$

Practically, the optimal level allocation Λ_{kl}^* should be given by $\Lambda_{kl}^* = \max(1, \lfloor \Lambda_{kl} \rfloor)$, a measure that automatically prevents the allocation of negative numbers of bits. Obviously this step must be followed by re-normalization of the bit allocation in order to comply with the bits budget constraint. $\mathcal{K}$ can be taken from 1 to 3, whereas Ω will be $\{(k,l)|k + l \leq 7,\ k, l = 0, 1, ..7\}$, simulating the standard JPEG approach which is coding of 8×8 transform coefficients, emphasizing the low frequency range via the precise encoding of only about $|\Omega| = 36$ coefficients.

Using the above described parameter ranges, we plot the predictions of the analytical model for the expected mean square error as a function of the slicings M with bit usage as a parameter. Figures 2 and 3 demonstrate the approximated error as a function of the number of slicings for various total number of bits. Figure 2 displays the predictions of the theoretical model in conjunction with optimal level allocation while Figure 3 uses the JPEG style rigid relative bit allocation. In both figures the left side shows the results of restricting the number of bits or quantization levels to integers, while the right side shows the results allowing fractional bit and level allocation.

These figures show that for every given total number of bits there is an optimal slicing parameter M indicating the optimal scaling factor. Note that the integer allocation cause in both cases non-smooth behaviour. Also, in Figure 2 it appears that the

minimum points are local ones and the error tends to decrease as M increases. This phenomenon can be explained by the fact that we used an approximation of the quantization error which fails to predict the true error for a small number of bits at large scales.

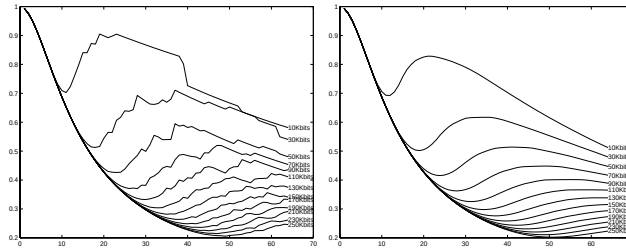

Fig. 2. Theoretical prediction based on optimal level allocation MSE versus number of slicings M with total bits usage as a parameter. Here, we used the typical values $\alpha = 150$, and $k = 3$.

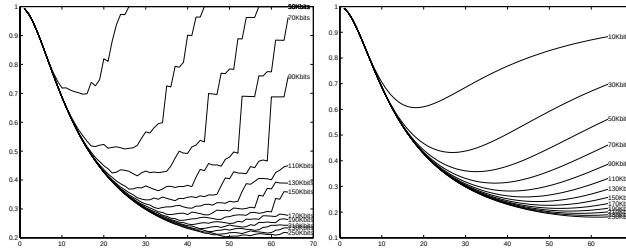

Fig. 3. Rigid relative bit allocation based prediction of MSE versus number of slicings M with total bits usage as a parameter. Here, we used the typical values $\alpha = 150$, and $k = 1$.

Figure 4 shows the theoretical prediction of PSNR versus bits per pixel curves for typical 512×512 images with different scales (different values of M, where scale$= 8M/512$). One may observe that the curve intersections occur at similar locations as those of the experiments with real images shown in the next section.

5 Compression Results for Natural and Synthetic Images

In order to verify the validity of the analytic model and design a system for image transcoding we generate synthetic images for which the autocorrelation is similar to

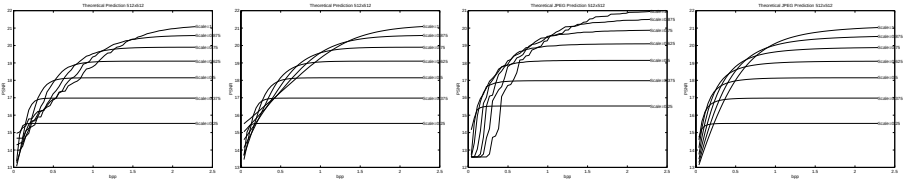

Fig. 4. Theoretical (two left frames) and rigid relative (two right frames) bit allocation based prediction of PSNR versus bits per pixel with image scaling as a parameter. Again, we used the typical values $\alpha = 150$, and $\kappa = 3$ for the theoretical prediction case, and $\kappa = 1$ for the JPEG-style case.

that of a given image. Next, we plot the PSNR/bpp JPEG graphs for all JPEG qualities, one graph for each given scaling ratio. The statistical model is considered valid if the behaviour is similar for the natural image and the synthesized one.

5.1 Image Synthesis

Assume that an image $g(m,n)$ autocorrelation function is that of a homogeneous random field of the form

$$R_{gg}(m,n) = \frac{1}{MN}\sum_{m'=0}^{M-1}\sum_{n'=0}^{N-1} g(m',n')g(m'+m,n'+n) = e^{-\alpha_x|m|-\alpha_y|n|}.$$

Define the Fourier transform $\hat{g}(k) = \mathcal{F}\{g(x)\}$. Then, the power spectrum of the real signal is given by $\mathcal{F}\{R_{gg}(x)\} = P_{gg}(k) = \langle \hat{g}(k)\hat{g}^*(k)\rangle$. Now, considering the $1D$ signal with the above given statistics, we have $\langle \hat{g}(k)\hat{g}^*(k)\rangle = \mathcal{F}\{e^{-\alpha|x|}\} = \frac{2\alpha}{\alpha^2+k^2}$. Thus, we have that $\hat{g}(k) = \sqrt{2\alpha}\frac{\alpha-ik}{\alpha^2+k^2}$, and

$$\begin{aligned} g(x) \equiv \mathcal{F}^{-1}\{\hat{g}(k)\} &= \mathcal{F}^{-1}\left\{\sqrt{\frac{\alpha}{2}}\frac{2\alpha}{\alpha^2+k^2}\right\} + \mathcal{F}^{-1}\left\{-\frac{1}{\sqrt{2\alpha}}ik\frac{2\alpha}{\alpha^2+k^2}\right\} \\ &= \sqrt{\frac{\alpha}{2}}e^{-\alpha|x|} - \frac{1}{\sqrt{2\alpha}}\frac{d}{dx}e^{-\alpha|x|} = \sqrt{\frac{\alpha}{2}}e^{-\alpha|x|}(1+\mathrm{sgn}(x)) \\ &= \begin{cases} \sqrt{2\alpha}e^{-\alpha|x|} & x > 0 \\ 0 & x \le 0 \end{cases} \end{aligned}$$

In order to generate synthetic images, we 'color' a uniform random (white) noise as follows. Let g_n be an $M \times N$ matrix in which each entry is a uniformly distributed random number. Next, let p and q be $M \times N$ matrices with elements

$$p(m,n) = \begin{cases} \sqrt{2\alpha_x}e^{-\alpha_x m} & n = \frac{N}{2}, m = 1,...,M \\ 0 & \text{otherwise,} \end{cases},$$

$$q(m,n) = \begin{cases} \sqrt{2\alpha_y}e^{-\alpha_y n} & m = \frac{M}{2}, n = 1,...,N \\ 0 & \text{otherwise.} \end{cases}$$

Our synthetic image is generated by the process $g(m,n) = \mathcal{F}_{2D}^{-1}\{\mathcal{F}_{2D}\{g_n\} \cdot \mathcal{F}_{2D}\{p\} \cdot \mathcal{F}_{2D}\{q\}\}$.

5.2 Estimating the Image Statistics α_x and α_y

In order to generate a synthetic image with the same statistics as that of the natural one, we have to first estimate the properties of the given image. Let us present a simple method for estimating the image statistics. We already used the relation $\mathcal{F}_{2D}\{R_{gg}(x,y)\} = P_{gg}(k,l) = \langle \hat{g}(k,l), \hat{g}^*(k,l)\rangle$. Explicitly, for our statistical image model we have that the power spectrum and the autocorrelation are given by

$$\frac{2\alpha_x}{\alpha_x^2+k^2}\frac{2\alpha_y}{\alpha_y^2+l^2} = \langle \hat{g}(k,l), \hat{g}^*(k,l)\rangle, \qquad e^{-\alpha_x|x|-\alpha_y|y|} = \mathcal{F}_{2D}^{-1}\{\langle \hat{g}(k,l), \hat{g}^*(k,l)\rangle\}.$$

Thus, all we need to do is to estimate the slopes of the plane given by

$$\begin{aligned}\alpha_x|x| + \alpha_y|y| &= -\ln(\mathcal{F}_{2D}^{-1}\{\langle \hat{g}(k,l), \hat{g}^*(k,l)\rangle\}) \\ &= -\ln(\mathcal{F}_{2D}^{-1}\{\langle \mathcal{F}_{2D}\{g(x,y)\}, (\mathcal{F}_{2D}\{g(x,y)\})^*\rangle\}).\end{aligned}$$

This was the estimation implemented in our experiments.

5.3 Experimental Results

A JPEG compression performance comparison for a natural image and its random synthesized version is shown in Figure 5 for a 256×256 image (first row) and 512×512 image (second row). The figures show the compression results of synthetic versus natural images with similar statistics. Synthetic and original images and their corresponding autocorrelations are presented with their corresponding JPEG PSNR/bpp compression curves for 4 scales. The above experiments indicate that the crossing locations between scales in the synthetic images appear to be a good approximation of the crossings in the natural images. Thus, based on the second order statistics of the image we can predict the optimal scale factor. Moreover, the non-stationarity nature of images have a minor impact on the optimal scale factor. This is evident from the alignment of the results of the natural and the synthetic images. There appears to be a vertical gap (in PSNR) between the synthetic and the natural images. However, similar PSNR gaps appear also between different synthetic images.

6 Conclusions

We have presented an analytical model and a set of empirical results verifying our model and support the idea of scaling before transform coding for optimal compression. The numerical results prove the validity of the model, and the simple algorithms we introduced can be used in an on-line system, to (i) extract the image statistical coefficients (α_x and α_y). Next, (ii) use the image statistics, size, and bits budget to decide on the optimal scaling, e.g. for the JPEG compression in a transcoding system. In another report we will explore extensions and implementation issues, like extracting the image statistical characteristics from the JPEG DCT coefficients in an efficient way, obtaining second order statistics locally and using an hierarchical slicing of the image to various block sizes, and more.

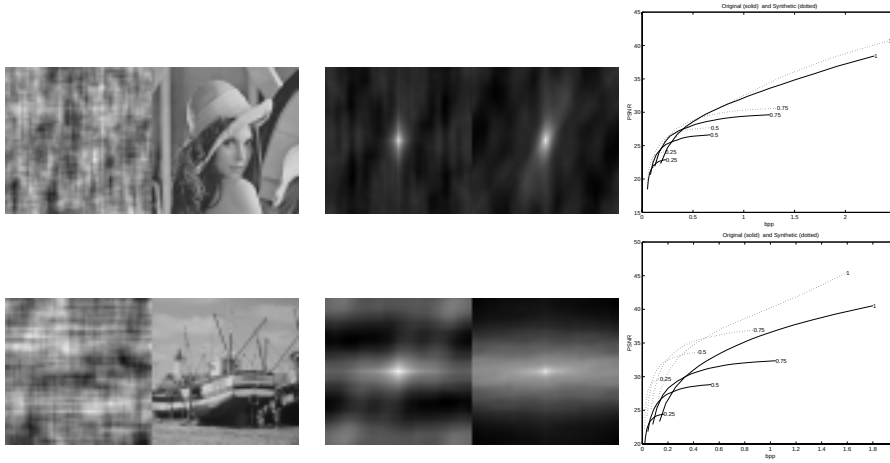

Fig. 5. Comparison between a natural and a synthesized image with similar autocorrelation.

References

1. W.B. Pennebaker and J.L. Mitchell. *JPEG Still Image Compression Standard.* Van Nostrand Reinhold, New York. 1992.
2. D. Taubman. High Performance Scalable Image Compression with EBCOT, *IEEE Trans. on Image Processing,* 9(7):1158–1170 2000.
3. A. Gersho and R.M. Gray. *Vector Quantization and Signal Compression,* Kluwer Academic,1992
4. A. Bruckstein. On Optimal Image Digitization *IEEE Trans. ASSP*, 35(4):553-555, 1987.
5. A. Bruckstein. On Soft Bit Allocation, *IEEE Trans. ASSP* 35(5):614-617, 1987.
6. A.K.Jain. *Fundamentals of Digit Image Processing,* Prentice Hall, 1989